

The Effect of Milling Time and Sintering Temperature on Crystallization of BaFe₁₂O₁₉ Phase and Magnetic Properties of Ba-Hexaferrite Magnet

G. SADULLAHOĞLU^{a,*}, B. ERTUĞ^b, H. GÖKÇE^b, B. ALTUNCEVAHIR^c, M. ÖZTÜRK^d,
R. TOPKAYA^d, N. AKDOĞAN^d, M.L. ÖVEÇOĞLU^b AND O. ADDEMİR^b

^aBulent Ecevit University, Metallurgical and Materials Engineering Department, 67100, Zonguldak, Turkey

^bIstanbul Technical University, Metallurgical and Materials Engineering Department, 34469, Istanbul, Turkey

^cIstanbul Technical University, Physics Engineering Department, 34469, Istanbul, Turkey

^dGebze Institute of Technology, Department of Physics, 41400 Gebze, Kocaeli, Turkey

(Received April 2, 2014; in final form June 15, 2015)

Barium hexaferrite samples were prepared by mechanical alloying using the stoichiometric amounts of BaCO₃ and Fe₂O₃ precursors followed by heat treatment applied in the temperature range 700–1150 °C. It was found that the high energy ball mill with a milling rate enabled to obtain powders with the finer particles at the reduced milling time mechanical alloying of the initial powders linked to the formation of barium hexaferrite phase. The exothermic reaction peaks corresponding to the formation of BaFe₁₂O₁₉ phase shift from 928 °C to 793 °C for the increased milling time up to 6 h. This was resulted in improved magnetic properties that the M_s value of the as-blended sample sintered at 800 °C risen from 31.16 emu/g to 53.46 emu/g after milling for 6 h. The saturation magnetization and remanence values of the samples mechanically alloyed for 3 h and sintered at 1150 °C also increased to 63.57 emu/g and 31.26 emu/g, respectively, more than for 800 °C and 900 °C. The increase in the annealing temperature favours the formation of BaFe₁₂O₁₉ phase in the samples.

DOI: [10.12693/APhysPolA.128.377](https://doi.org/10.12693/APhysPolA.128.377)

PACS: 75.50.Vv, 75.60.Ej

1. Introduction

Barium ferrite has the formula of BaO·6Fe₂O₃, a hexagonal crystal structure, and fairly large uniaxial crystal anisotropy. The hexagonal c axis is the easy axis and the crystal anisotropy constant K is 3.3×10^6 erg/cm³ or 330 kJ/m³. The M_s is 380 emu/cm³ or 72 emu/g at room temperature and the Curie point is 450 °C. The hexagonal unit cell of barium ferrite contains 64 atoms, the Ba²⁺ and O²⁻ ions both are nonmagnetic, the magnetic Fe³⁺ ions are ferromagnetic, each will a moment of $5 \mu_B$. The Fe³⁺ ions have their moments normal to the plane of the oxygen layers, and thus has parallel or antiparallel to the c axis of the hexagonal cell, which is $\langle 0001 \rangle$ direction [1–3]. Besides their high Curie temperature, high coercivity as well as excellent corrosion resistivity, barium hexaferrites are fabricated due to ease of processing and low cost of raw materials, which makes them technologically attractive permanent magnetic material most widely used in the fabrication of magnetic and magneto-optic recording and microwave devices [4–7].

High saturation magnetization, sufficient coercivity and structural stability are important criteria for a permanent magnet. It is known that high coercivities require fine structures, with a particle size significantly

small about 1 μm . There are several techniques to produce fine particle barium hexaferrites, which are coprecipitation [8] glass crystallization [9], mechanochemical activation [10] and mechanical alloying [11, 12]. High-energy mechanical milling (mechanical alloying) is a simple technique used to obtain high coercive hexaferrites associated with fine microstructure. By utilizing this process, the particle size can be reduced from multidomain to a single domain by using different milling processes to reach high coercivities up to 6–7 kOe and high saturation magnetization about 75 emu/g [13, 14]. BaM-hexaferrite produced by high energy ball mill (HEBM) indicated superior magnetic properties over the ceramics prepared by conventional solid-state reaction for magnetic recording applications [15, 16].

However, HEBM as a prevalent technique requires a comprehensive synthesis of M-type hexaferrites prepared by HEBM powders, because a systematic investigation on this process and effects on magnetic properties are still missing in the literature.

Therefore, in the present study, Ba-hexaferrite powders were prepared by high energy ball milling for different periods, thermal reactions of the milled powders were determined by differential thermal analysis (DTA) analysis. The influences of the process on the reaction temperature, phase formation, magnetic structure and magnetic properties were investigated.

*corresponding author; e-mail: gsadullahoglu@beun.edu.tr

2. Experimental procedure

Barium carbonate (BaCO_3) powders (MerkTM, mean particle size: 319.3 nm) and iron oxide (Fe_2O_3) (DETSANTM, mean particle size: 1.60 μm) were blended and mixed in a molar ratio of Fe/Ba: 1/12. The amounts of prepared powder batches weighed in a XB320M (PrecisaTM, Dietikon) sensitive balance were 5–6 g. HEBM (mechanical alloying) were carried out in a vibrating ball mill (SpexTM 8000 D Mixer/Mill) with a speed of 1200 rpm in a hardened steel vial (50 ml capacity) and hardened stainless steel balls with a diameter of 6.35 mm (1/4 in.) with a ball-to-powder weight ratio (BPR) of 10:1. Mechanical alloying duration varied from 3 h to 20 h. Stearic acid was used as the process control agent (PCA) to minimize cold welding between powder particles and thereby to inhibit agglomeration. Milling was not interrupted and at the end of mentioned durations, mechanically alloyed (MA'd) powders were unloaded under air. The mechanically alloyed powders were cold pressed into pellets with a diameter of 12 mm. Cold pressed samples were annealed for 1 h at the temperatures of 800 °C, 900 °C, 1150 °C under air. Exothermic reactions were determined by differential thermal analysis (DTA) analysis by heating the as-blended and milled powders up to 1200 °C with the heating rate of 10 °C/min in air. The phase compositions of the milled powders and the sintered samples were performed by X-ray diffraction (XRD) technique using a D8 Advanced Series Powder Diffractometer (BrukerTM) with $\text{Cu } K_\alpha$ (1.54060 Å) radiation in the 2θ range of 20–80° with 0.02° steps at a rate of 1°/min. International Centre for Diffraction Data® (ICDD) powder diffraction files were utilized for the identification of crystalline phases. Density measurements of the sintered pellets were determined by the Archimedes method. The annealed bulk samples were covered by wax before the measurements and the volume of the wax was taken into account in the calculations. For the magnetic measurements the bulk samples were cut in rectangular shape with a long edge to short edge ratio of about 2. The external magnetic field was applied along the long axis of the specimens. Magnetic properties of the barium hexaferrite samples were measured by vibrating sample magnetometer (VSM) PPMS9T system of Quantum DesignTM with an applied field up to 40 kOe at room temperature.

3. Results and discussions

Figure 1 shows the XRD patterns of the BaCO_3 and Fe_2O_3 powders MA'd at different durations. The XRD pattern of as-blended powders (Fig. 1a) reveals the presence of the characteristic peaks of the BaCO_3 (Bravais lattice: primitive orthorhombic, space group: $Pnma$; $a = 0.646$ nm, $b = 0.522$ nm, $c = 0.883$ nm) [17] hematite (Fe_2O_3) phase (the Bravais lattice: rhombohedral, space group: $R\bar{3}c$; $a = b = 0.542$ nm, $c = 1.371$ nm) [18] and the diffraction peak reflected from the (119) diffraction plane belongs to maghemite (Fe_2O_3)

phase at $2\theta = 35.86^\circ$ detected in the XRD measurements of initial Fe_2O_3 powders (the Bravais lattice: primitive tetragonal, $a = b = 0.834$ nm, $c = 2.502$ nm) [19].

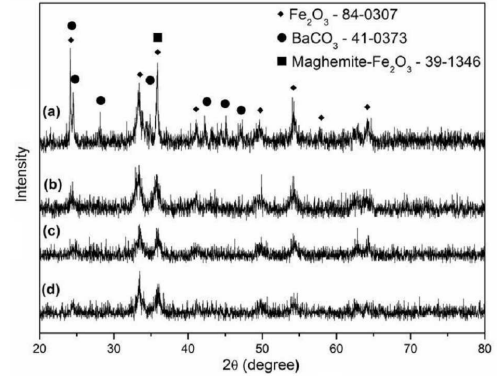


Fig. 1. XRD patterns of the as-blended (a), MA'd for 6 h (b), 12 h (c), and 20 h (d).

Two diffraction peaks which are reflected from the (110) diffraction plane of the hematite phase and the reflection from (119) plane belonging to the maghemite phase overlapped at $2\theta = 34.85^\circ$ (Fig. 1a). Figure 1b–d shows a significant decrease in the intensity of this peak with increasing MA duration which might be due to transformation of maghemite phase into hematite by mechanical alloying of the initial powders. Furthermore, the increased milling time caused the broadening of the diffraction lines of the mixed Fe_2O_3 and BaCO_3 powders (Fig. 1a–c). Any reflections to the hard magnetic $\text{BaFe}_{12}\text{O}_{19}$ phase were not detected in the XRD spectra of the milled powders (Fig. 1).

Figure 2 displays the XRD patterns of the samples as blended and MA'd for different times (3–20 h) and heat treated at 700 °C for 1 h. The main peaks reflected from all the specimens belong to the Fe_2O_3 phase and any diffraction peaks of $\text{BaFe}_{12}\text{O}_{19}$ were not detected in the XRD spectra of the specimens. A small peak from an intermediate phase of $\text{Ba}_2\text{Fe}_6\text{O}_{11}$ (the Bravais lattice: primitive orthorhombic, space group: $Pnmm$; $a = 2.302$ nm, $b = 0.518$ nm, $c = 0.89$ nm) [20] was reflected from the samples milled for 3 h and 6 h. Further milling of the powders leads to the broadening of the peaks, small reflections from the BaO_2 phase (the Bravais lattice: body centered tetragonal, space group: $I4/mmm$; $a = b = 0.378$ nm, $c = 0.677$ nm) [21] were detected in the sample as blended, it can be said that BaCO_3 phase were partially transformed to the BaO_2 after annealing of the mixed powders.

DTA of the as-blended and MA'd powders for 3, 6, 9, and 20 h are presented in Fig. 3. Two initial exothermic peaks were observed for the milled powders at about 230 °C and 282 °C, respectively. The curve belonging to the as-milled sample shows an exothermic peak at about 928 °C pertaining to the decomposition temperature of the precursors into the hexaferrite phase. The exothermic peaks shifted from 928 °C to 793 °C for

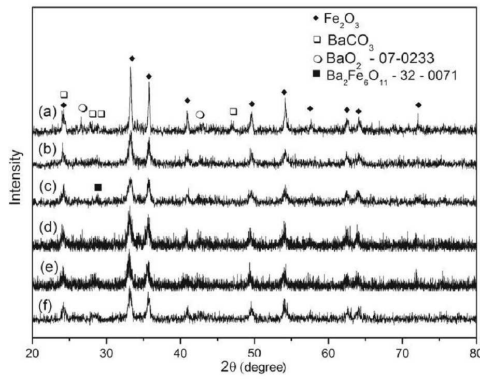


Fig. 2. XRD patterns of the samples (a) as blended, (b) MA'd for 3 h, (c) 6 h, (d) 9 h, (e) 12 h and (f) 20 h and sintered at 700 °C for 1 h.

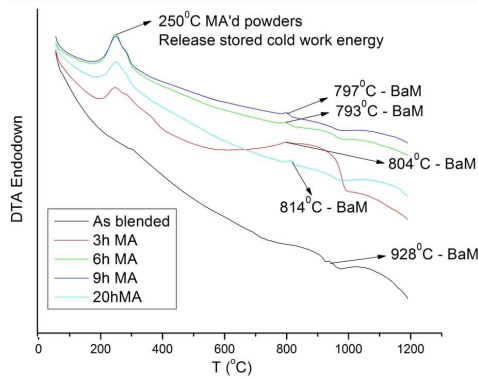


Fig. 3. DTA patterns of as-blended and MA'd Fe_2O_3 and BaCO_3 powders.

the increased milling durations as a result of more reactive surface of the powders to form $\text{BaFe}_{12}\text{O}_{19}$ hard magnetic phase with the finer particles. In a reported study, after the milling of the initial powders for 30 h by using high energy ball mill with 300 rpm this exothermic peak temperature was 834 °C [15]. In our study, this temperature decreased to 804 °C for the sample milled for 3 h by using high energy ball mill with 1200 rpm.

TABLE

Exothermic reaction temperatures of as blended and MA'd powders.

Milling time [h]	Reaction temperature [°C]
as blended	928
3 h MA	804
6 h MA	793
9 h MA	797
12 h MA	801
20 h MA	814

On the other hand, Table shows that the exothermic peak temperature increased for the powders MA'd for 9 h

and 20 h which may be attributed to the created internal strains and defects by overmilling.

In order to identify the initial exothermic peaks between 230 °C and 300 °C for the samples milled between 3 h and 20 h, an XRD investigation (Fig. 4) was carried out on the powders MA'd for 6 h and annealed at 500 °C for 5 h. The XRD pattern of the annealed sample revealed the diffraction peaks of the BaFeO_3 phase (the Bravais lattice: rhombohedral; space group: $R-3m$; $a = b = 0.569$ nm, $c = 2.801$ nm) [22]. The milling process might enable the formation of this phase at low temperature associated with the increased reactive surface of the powders. Figure 4b shows a small increase in the intensities of the BaCO_3 and Fe_2O_3 phases. The release of the cold work energy in the system stored during the mechanical alloying process might be another factor for the initial exothermic peaks of MA'd powders at low temperatures. Figure 3 displays endothermic peaks for the samples between 850 °C–1000 °C, this might be most probably due to the growth of the crystals belonging to the formed magnetic $\text{BaFe}_{12}\text{O}_{19}$ phase.

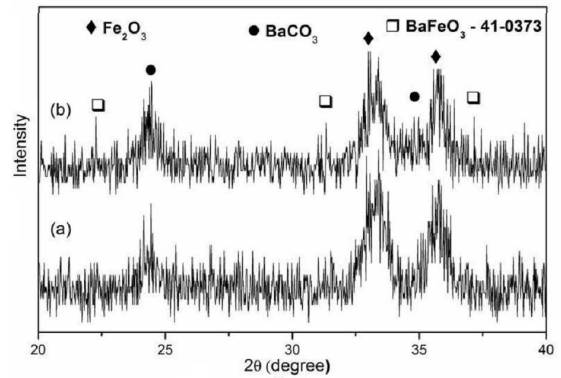


Fig. 4. XRD patterns of the sample (a) MA'd for 6 h and (b) annealed at 500 °C for 5 h.

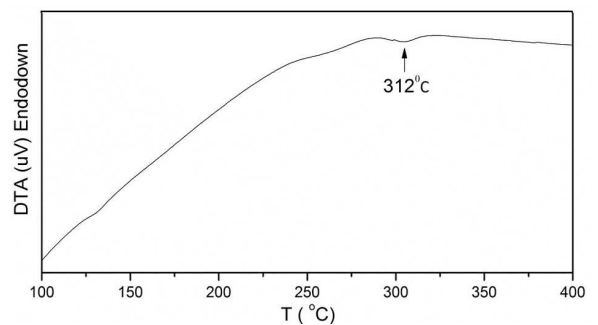


Fig. 5. DTA patterns of Fe_2O_3 powders MA'd for 6 h.

Figure 5 shows DTA measurement of the Fe_2O_3 powders milled for 6 h. The endothermic reaction peak observed at about 312 °C may belong to the transformation of maghemite into hematite since the reduction of particle size creates more reactive surface of the powders to form a

new phase. Because in a dry state, maghemite depending on its origin and the content of foreign ions, transforms to hematite in the temperature range 370–600 °C [23].

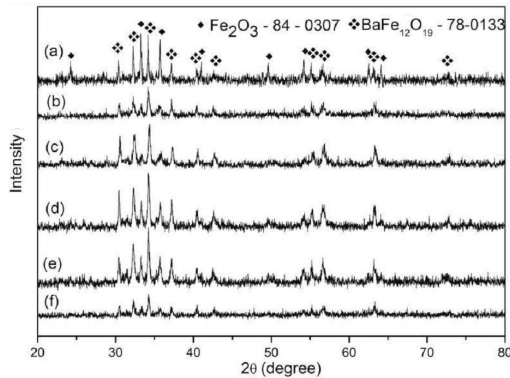


Fig. 6. XRD patterns of the samples (a) as blended, (b) MA'd for 3 h, (c) 6 h, (d) 9 h, (e) 12 h and (f) 20 h and sintered at 800 °C for 1 h.

Figure 6 shows the XRD patterns of the samples as blended and milled at different durations (3–20 h) and annealed at 800 °C for 1 h revealing the peaks belonging to the Fe_2O_3 phase and $\text{BaFe}_{12}\text{O}_{19}$ phase (the Bravais lattice: simple hexagonal; space group: $P63/mmc$; $a = b = 0.586$ nm, $c = 2.309$ nm) [24]. The diffraction peaks of this intermediate phase disappeared after heat treatment as shown in Fig. 6f. For all samples, the formation of the magnetic $\text{BaFe}_{12}\text{O}_{19}$ hard ferrite phase was not completed after the heat treatment at 800 °C for 1 h. The main peaks diffracted from the as-blended sample belong to the Fe_2O_3 phase in accordance with the exothermic peak temperature to form hard magnetic $\text{BaFe}_{12}\text{O}_{19}$ phase observed in the DTA analysis (Fig. 3). According to the DTA thermograph, the exothermic reaction temperature is 928 °C for the as-blended sample and 800 °C is not enough to obtain pure hard magnetic $\text{BaFe}_{12}\text{O}_{19}$ phase. The diffraction peaks of the $\text{BaFe}_{12}\text{O}_{19}$ phase increased sharply after milling for 3 h. Similar peaks were observed at the same annealing temperature for the 15 h milled sample annealed at the same temperature as reported by Jin et al. [25].

Figure 7 shows the XRD investigations of the samples milled for 3 h and annealed at 800 °C, 900 °C and 1150 °C for 1 h. The diffraction peaks of the hard magnetic $\text{BaFe}_{12}\text{O}_{19}$ phase were observed in the samples milled for 3 h and sintered at 800 °C and 900 °C with the presence of the peaks reflected from the Fe_2O_3 phase. The intensities of peaks which belong to the Fe_2O_3 phase decreased with increasing annealing temperature and disappeared after sintering at 1150 °C. The influences of annealing temperature and milling time on the magnetic properties of the $\text{BaCO}_3 + 6\text{Fe}_2\text{O}_3$ powders are shown in Fig. 8a–c. The lowest values of the saturation magnetization and coercivity were exhibited by the as-milled samples heat treated at 800 °C. This can be attributed to incomplete formation of $\text{BaFe}_{12}\text{O}_{19}$ hard ferrite phase

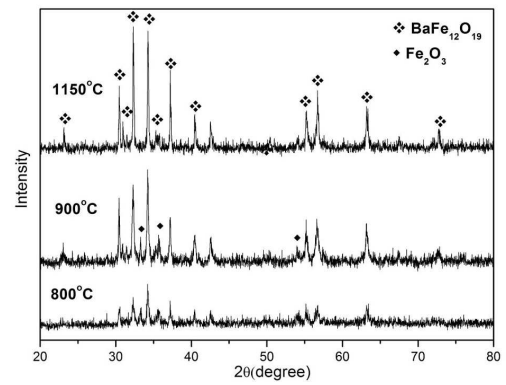


Fig. 7. X-ray diffraction patterns of the samples MA'd for 3 h and sintered at different temperatures.

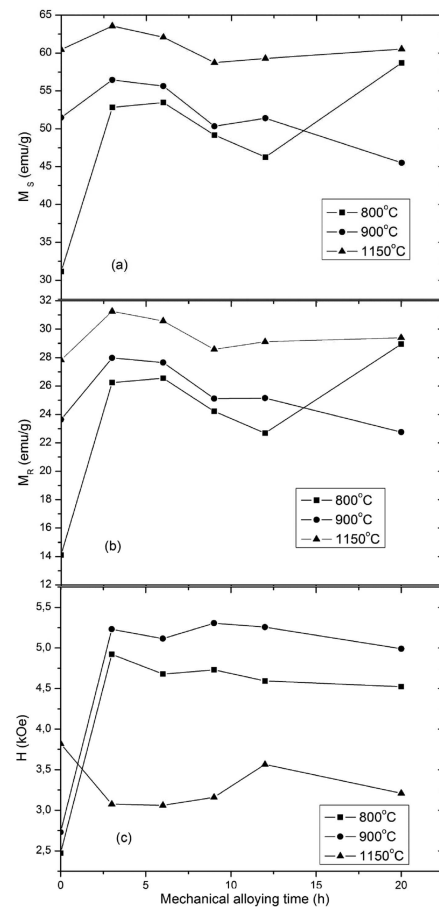


Fig. 8. Magnetic properties of the mechanically alloyed samples sintered at different temperatures for 1 h.

with the presence of Fe_2O_3 which has a major diffraction peak detected in the XRD diffraction analysis in Fig. 6a. This antiferromagnetic phase is detrimental to the magnetic properties of the sample. In Fig. 8a and b, the saturation magnetization and remanence of the samples mechanically alloyed for 3 h and sintered at 1150 °C reached the maximum values of 63.57 emu/g and 31.26 emu/g respectively more than that annealed at 800 °C and 900 °C, because the higher annealing temperature favoured the

formation of $\text{BaFe}_{12}\text{O}_{19}$ crystallites in the samples during sintering process but at the expense of decrease in H_C due to the grain growth. Increase in milling time up to 6 h improved magnetic properties at low sintering temperatures of 800°C reflecting the increased amount of the hexaferrite phase in the composition. It is also consistent with the DTA results, due to the fact that the milled powders are already in activated state before annealing process because the increased milling time reduces the particle size and enhances the reactivity of the powders to enable the nucleation and growth of $\text{BaFe}_{12}\text{O}_{19}$ phase much faster than as-milled powders even at lower temperatures. But further milling durations lead to a small decrease in M_S and M_R values in accordance with the increase in the diffraction peaks reflected from the Fe_2O_3 phase (Fig. 6) as a result of the defects and internal strains which make hard the crystallization of the hexaferrite phase.

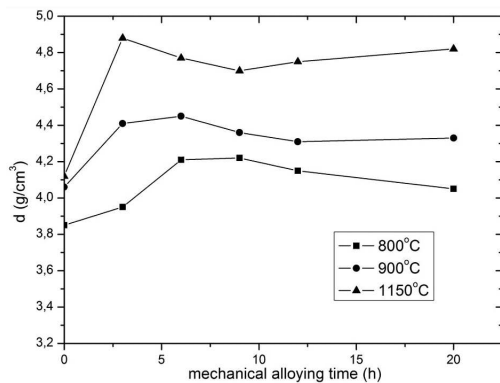


Fig. 9. Densities of the samples as blended and mechanically alloyed for different times and sintered at 800°C (a), 900°C (b) and 1150°C (c).

As shown in Fig. 8c for the as blended samples sintered at 1150°C , H_C has the highest value. This might be due to the presence of antiferromagnetic Fe_2O_3 phase on the grain boundaries which prevents the interaction of the magnetic $\text{BaFe}_{12}\text{O}_{19}$ grains as a result of the incomplete formation of the $\text{BaFe}_{12}\text{O}_{19}$ phase. It is due to the not well blended powders and the larger particles associated with the smaller reaction surface. Also the low density and porous structure may cause less interaction between magnetic $\text{BaFe}_{12}\text{O}_{19}$ grains. After milling for 3 h, H_C value increased sharply for the samples sintered at 800°C and 900°C , most probably due to the existence of antiferromagnetic Fe_2O_3 phase (Fig. 7) in the between hard magnetic $\text{BaFe}_{12}\text{O}_{19}$ grains and lower density values. However, H_C decreased for the sample sintered at 1150°C , it might be because that Fe_2O_3 phase disappeared in this sample as shown in Fig. 7 leading to an increase in hard ferrite phase ratio in the material. Thus, more magnetic $\text{BaFe}_{12}\text{O}_{19}$ grains in contact with each other result in higher M_S and M_R and lower H_C values. In addition, Fig. 9 showed that the highest density value belongs to the samples sintered at 1150°C leading to high magnetization and low coercivity because of the

existence of demagnetization fields created in pores in the magnetic material.

The highest coercivity is 5.31 kOe for the sample annealed at 900°C and mechanically alloyed for 9 h, it decreased to 4.99 kOe for 20 h, probably due to the lower formation of barium hexaferrite phase. In an early report, H_C is 279 kA/m (about 3.5 kOe) observed as for 50 h mechanical alloying time and at the same annealing temperature [26]. In another study, H_C is in the range 5–5.5 kOe obtained between 750°C and 1000°C for 24 h milling time, by using SPEX 8000 mixer/mill for milling of powders [13].

In addition, it was observed that the influence of milling duration on the formation of Ba hexaferrite phase and magnetic properties of the samples decreases with the increase of the sintering temperature.

The density measurements of the pellets sintered at various temperatures and milled for different times are given in Fig. 9. As shown in the figure sintering temperature influences significantly on the densities of the samples. Theoretical density of $\text{BaFe}_{12}\text{O}_{19}$ is 5.3 g/cm^3 .

The density of the pellets sintered at 800°C has the lowest value 3.85 g/cm^3 which increases up to 4.22 g/cm^3 for the sample mechanically alloyed for 9 h, further milling time decrease the density values since defects created by milling process. The highest measured density is 4.88 g/cm^3 for the sample mechanically alloyed for 3 h and heat treated at 1150°C which has the highest saturation magnetization (M_S) value because of the increase in hard magnetic material per unit volume of the sample.

4. Conclusions

1. The formation temperature of the barium hexaferrite phase is closely related to the milling process. It was observed that the higher milling rate enables to obtain powders with finer particles at the reduced mechanical alloying durations linked to the formation of $\text{BaFe}_{12}\text{O}_{19}$ phase. The exothermic peak temperature represented by the decomposition of the precursors to form hexaferrite phase decreased significantly with the increase in milling time from 928°C for the as-milled sample to 793°C to the milled sample for 6 h by using high energy ball mill with 1200 rpm. This is also confirmed by the XRD analysis and magnetic properties of the samples annealed and milled for 6 h and sintered at 800°C for 1 h. The main peaks diffracted from the as-blended sample belong to the Fe_2O_3 phase in Fig. 6 and M_S value of the as-blended sample rose from 31.16 emu/g to 53.46 emu/g after milling for 6 h.
2. The highest M_S value of 63.57 emu/g was measured for the sample mechanically alloyed for 3 h and sintered 1150°C for 1 h. The highest H_C value is 5.31 kOe obtained for the sample milled for 9 h

and heat treated at 900°C for 1 h, but the magnetization is 50.33 emu/g which is lower than that sintered at 1150°C because of the presence of the antiferromagnetic hematite (Fe₂O₃) phase in the material.

3. Any reflections to the hard magnetic BaFe₁₂O₁₉ phase were not detected in the XRD spectra of the specimens sintered at 700°C for 1 h (Fig. 2).
4. Magnetization values increase gradually with the increases in sintering temperatures and mechanical alloying durations up to 6 h, because overmilling causes defects and internal stresses in the crystal structure which deteriorate the magnetic properties of the sample. On the other hand, the effect of mechanical alloying duration on the formation of Ba hexaferrite phase and magnetic properties of the samples decreases with the increase of the sintering temperature.

Acknowledgments

We would like to express our gratitude to State Planning Organization (DPT) for funding the project entitled “Advanced Technologies in Engineering” with the project number 2001K120750 out of which the main infrastructure of the Particulate Materials Laboratories was founded. This work was partially supported by DPT (State Planning Organization of Turkey) through the Project no. 2009K120730 (Nanomagnetism and Spintronics Reseach Center-NASAM of Gebze Institute of Technology) and TÜBİTAK through the Project no. 209T061.

References

- [1] B.D. Cullity, C.D. Graham, *Introduction to Magnetic Materials*, Wiley, New Jersey, USA 2009, p. 190.
- [2] R. Smolinski, J.M.D. Coey, *Permanent Magnetism*, Bookcraft, UK 1999, p. 261.
- [3] A. Goldman, *Modern Ferrite Technology*, 2nd ed., Springer, New York 2006, p. 104.
- [4] S.B. Narang, I.S. Hudiara, *J. Ceram. Process. Res.* **7**, 113 (2006).
- [5] K.K. Mallick, P. Shepherd, R.J. Green, *J. Europ. Ceram. Soc.* **27**, 2045 (2007).
- [6] J. Bursik, Z. Simsa, M. Cernansky, *J. Sol-Gel Sci. Technol.* **8**, 947 (1997).
- [7] S. Hussain, A. Maqsood, *J. Magn. Magn. Mater.* **316**, 73 (2007).
- [8] S.R. Janasi, M. Emura, F.J.G. Landgraf, D. Rodrigues, *J. Magn. Magn. Mater.* **238**, 168 (2002).
- [9] M. El-Hilo, H. Pfeiffer, K. O’Grady, W. Schüppel, E. Sinn, P. Görnert, M. Rösler, D.P.E. Dickson, R.W. Chantrell, *J. Magn. Magn. Mater.* **129**, 339 (1994).
- [10] O. Abe, M. Narita, *Solid State Ion.* **101**, 103 (1997).
- [11] A. Gonzales-Angeles, G. Mendoza-Suarez, A. Gruskova, R. Dosoudil, R. Ortega Zempoalteca, *Mater. Lett.* **58**, 2906 (2004).
- [12] S. Wang, J. Ding, Y. Shi, Y.J. Chen, *J. Magn. Magn. Mater.* **219**, 206 (2000).
- [13] J. Ding, D. Maurice, W.F. Miao, P.G. McCormick, R. Street, R. Street, *J. Magn. Magn. Mater.* **150**, 417 (1997).
- [14] J. Ding, H. Yang, W.F. Miao, P.G. McCormick, R. Street, R. Street, *J. Alloys Comp.* **221**, 70 (1995).
- [15] P. Sharma, R.A. Rocha, S.N. de Medeiros, A. Paesano Jr., *J. Alloys Comp.* **443**, 37 (2007).
- [16] D. Lisjak, M. Drogenik, *J. Europ. Ceram. Soc.* **24**, 1841 (2004).
- [17] Powder Diffraction Files: Card No. 41-0373, database edition, The International Center for Diffraction Data (ICDD).
- [18] Powder Diffraction Files: Card No. 84-0307, database edition, The International Center for Diffraction Data (ICDD).
- [19] Powder Diffraction Files: Card No. 39-1346, database edition, The International Center for Diffraction Data (ICDD).
- [20] Powder Diffraction Files: Card No. 73-1739, database edition, The International Center for Diffraction Data (ICDD).
- [21] Powder Diffraction Files: Card No. 07-0233, database edition, The International Center for Diffraction Data (ICDD).
- [22] Powder Diffraction Files: Card No. 85-0852, database edition, The International Center for Diffraction Data (ICDD).
- [23] R.M. Cornell, U. Schwertmann, *The Iron Oxides*, Wiley-VCH, Weinheim 2003, p. 382.
- [24] Powder Diffraction Files: Card No. 78-0133, database edition, The International Center for Diffraction Data (ICDD).
- [25] Z. Jin, W. Tang, J. Zhang, H. Lin, Y. Du, *J. Magn. Magn. Mater.* **182**, 231 (1998).
- [26] R. Nowosielski, R. Babilas, G. Dercz, L. Pajak, W. Skowronski, *J. Achiev. Mater. Manufact. Eng.* **27**, 51 (2008).